Probing Time Reversal Symmetry Breaking Topological Superconductivity in Twisted Double Layer Copper Oxides with Polar Kerr Effect

Oguzhan Can[1,*] Xiao-Xiao Zhang[1,2,*] Catherine Kallin,[3] and Marcel Franz[1]

[1]*Department of Physics and Astronomy and Stewart Blusson Quantum Matter Institute, University of British Columbia, Vancouver, British Columbia V6T 1Z4, Canada*
[2]*RIKEN Center for Emergent Matter Science (CEMS), Wako, Saitama 351-0198, Japan*
[3]*Department of Physics and Astronomy, McMaster University, Hamilton, Ontario L8S 4M1, Canada*

Recent theoretical work predicted the emergence of a chiral topological superconducting phase with spontaneously broken time reversal symmetry in a twisted bilayer composed of two high-T_c cuprate monolayers such as $Bi_2Sr_2CaCu_2O_{8+\delta}$. Here, we identify a large intrinsic Hall response that can be probed through the polar Kerr effect measurement as a convenient signature of the $\mathcal{T}$-broken phase. Our modeling predicts the Kerr angle θ_K to be in the range of 10–100 μrad, which is a factor of 10^3 to 10^4 times larger than what is expected for the leading chiral superconductor candidate Sr_2RuO_4. In addition, we show that the optical Hall conductivity $\sigma_H(\omega)$ can be used to distinguish between the topological $d_{x^2-y^2} \pm id_{xy}$ phase and the $d_{x^2-y^2} \pm is$ phase, which is also expected to be present in the phase diagram but is topologically trivial.

Introduction.—While topological insulators and semi-metals appear to be abundant in nature [1], materials exhibiting topological superconductivity have been notoriously hard to find [2]. The leading candidate for the spin triplet $p_x + ip_y$ chiral superconductor, Sr_2RuO_4, which showed time reversal symmetry breaking (TRSB) in muon spin relaxation [3] and polar Kerr effect measurements [4], has been recently shown to be inconsistent with triplet pairing by Knight shift experiment [5]. Other suspected topological superconductors (TSCs) include $FeTe_xSe_{1-x}$ [6] and copper-doped Bi_2Se_3 [7], but at present the balance of evidence remains inconclusive. Perhaps the most convincing case for TSCs can be made in artificially engineered proximitized semiconductor quantum wires, where strong evidence for Majorana end modes has been reported by multiple groups and in a variety of experimental configurations [8–12].

In this Letter, we consider a platform recently proposed to artificially engineer a chiral topological superconductor based on a pair of monolayer thick cuprate superconductors assembled with a twist [13,14]. For a range of twist angles close to 45° such a bilayer is predicted to form a TRSB chiral phase that can be thought of as a $d_{x^2-y^2} \pm id_{xy}$ superconductor (which we abbreviate as $d \pm id'$ henceforth). We address here the pressing question of how such a topological $\mathcal{T}$-broken phase can be reliably identified in experiment. It is to be noted that a direct detection of the topological phase through its chiral edge modes is expected to be extremely challenging. In topological superconductors, these modes are neutral and must therefore be probed

via the *thermal* Hall effect, which is expected to attain a quantized contribution at low temperatures. Here, we show that, owing to its multiband nature and broken symmetries, the twisted bilayer exhibits strong anomalous *electrical* Hall conductivity that can be probed optically through a conventional polar Kerr effect (PKE) measurement.

The finite magneto-optic Kerr effect is a manifestation of time reversal symmetry breaking [15] in a material where linearly polarized incident light is reflected with elliptical polarization whose major axis is rotated with respect to the incident polarization axis. Kerr angle θ_K is directly related to the anomalous Hall conductivity $\sigma_H(\omega)$ defined below. TRSB is a necessary but not sufficient for finite Kerr rotation. In addition, any mirror reflection symmetry perpendicular to the incident wave vector must also be broken for $\sigma_H(\omega)$ to be nonzero [16]. In this work, we calculate the anomalous Hall conductivity of two stacked CuO_2 monolayers twisted with respect to one another by an angle close to 45°. Such a configuration develops a complex phase between the *d*-wave order parameters in the two layers, spontaneously breaking the time reversal symmetry as well as all mirror symmetries. The resulting system can be in a $d + id'$ or $d + is$ phase, depending on parameters such as doping and interlayer coupling strength [13]. Both phases break $\mathcal{T}$ and are fully gapped, but only the former exhibits topologically protected chiral edge modes. In this phase, we find a large intrinsic contribution to $\sigma_H(\omega)$ arising from interband transitions that involve chiral Cooper pairs—a mechanism originally identified in Ref. [17].

PKE and optical Hall conductivity.—In the presence of time reversal symmetry breaking, the polarization axis of a linearly polarized incident light will be rotated by the Kerr angle θ_K given by [18]

$$\theta_K(\omega) = \frac{4\pi}{2d\omega} \text{Im} \left[\frac{\sigma_H(\omega)}{n(n^2-1)} \right], \quad (1)$$

where n is the complex index of refraction, d denotes the separation of monolayer pairs, and $\sigma_H(\omega)$ is the antisymmetric part of the optical Hall conductivity per monolayer

$$\sigma_H(\omega) = \frac{1}{2} \lim_{q \to 0} [\sigma_{xy}(\boldsymbol{q}, \omega) - \sigma_{yx}(\boldsymbol{q}, \omega)]. \quad (2)$$

Equation (1) is valid when the sample thickness $h \gg \lambda$, the wavelength of the incident light. As such, it would apply to a stack composed of many bilayers. In the opposite limit $h \ll \lambda$, relevant to a single bilayer, the Kerr angle is given by a different expression [19], which in addition involves the longitudinal optical conductivity $\sigma_{xx}(\omega)$ and is specified in Eq. (8) below. Crucially, in both limits θ_K can be nonzero only when the Hall conductivity is finite. The latter can be computed from the Kubo formula as $\sigma_{xy}(\boldsymbol{q}, \omega) = (1/\omega)[\pi_{xy}(\boldsymbol{q}, \omega) - \pi_{xy}(\boldsymbol{q}, 0)]$. Here, ω is the frequency of the incident light and

$$\pi_{xy}(\boldsymbol{q}, \omega) = \int_0^\infty dt e^{i\omega t} \langle [\hat{J}_x^\dagger(\boldsymbol{q}, t), \hat{J}_y(\boldsymbol{q}, 0)] \rangle \quad (3)$$

is the current-current correlator. The total current operator $\hat{J}_i = e \sum_k \text{tr} \Psi_{\boldsymbol{k}}^\dagger \hat{v}_i \Psi_{\boldsymbol{k}}$ uses $\hat{v}_i = (\mathbb{1} \otimes \sigma_z) \partial_{k_i} h_{\boldsymbol{k}}^0$, where $h_{\boldsymbol{k}}^0$ and $h_{\boldsymbol{k}}^\Delta$ are the normal and superconducting parts of the system Bloch Hamiltonian $h_{\boldsymbol{k}} = h_{\boldsymbol{k}}^0 + h_{\boldsymbol{k}}^\Delta$, respectively, expressed in the orbital basis and σ_z acts in the particle-hole (Nambu) space. Under time reversal, the current correlator transforms as $\pi_{xy} \to \pi_{yx}$, while under mirror reflections along x or y axes $\pi_{xy} \to -\pi_{xy}$. Therefore, in order to obtain a nonzero Kerr effect, both time reversal and all mirror symmetries must be broken [16].

Equations (2) and (3) can be rewritten in terms of the eigenspectrum of $h_{\boldsymbol{k}}$ as

$$\sigma_H(\omega) = \frac{ie^2}{\omega} \sum_{\boldsymbol{k}, ab} \frac{(\omega + i\epsilon) Q_{ab}}{(E_{\boldsymbol{k}}^a - E_{\boldsymbol{k}}^b)^2 - (\omega + i\epsilon)^2} n_F(E_{\boldsymbol{k}}^a), \quad (4)$$

where a, b are band indices and $Q_{ab} = 2i \text{Im} \{v_{ab}^x v_{ba}^y\}_{\boldsymbol{k}}$ with the matrix element $v_{ab}^j = \langle a\boldsymbol{k} | \hat{v}_j | b\boldsymbol{k} \rangle$ computed from the Bloch eigenstates. This formulation is convenient for numerical calculations based on the lattice models of twisted bilayers discussed below. Details of the derivation are given in the Supplementary Material (SM) [20].

10-band model of coupled twisted copper oxide layers.— Following Ref. [13], we consider two stacked cuprate

monolayers twisted with respect to each other by a commensurate twist angle $\theta_{m,n} = 2 \arctan(m/n)$. Each CuO_2 plane is modeled by a minimal Hubbard model with nearest neighbor attractive potential, known to produce a $d_{x^2-y^2}$ superconductor within the standard Bogoliubov–de Gennes theory. The Hamiltonian has the form

$$H = -\sum_{ij,\sigma\alpha} t_{ij} c_{i\sigma\alpha}^\dagger c_{j\sigma\alpha} - \mu \sum_{i\sigma\alpha} n_{i\sigma\alpha}$$
$$+ \sum_{ij,\alpha} V_{ij} n_{i\alpha} n_{j\alpha} - \sum_{ij\sigma} g_{ij} c_{i\sigma1}^\dagger c_{j\sigma2}, \quad (5)$$

where $c_{i\sigma\alpha}^\dagger$ is the electron creation operator at site i with spin σ on the top (bottom) layer with index $\alpha = 1(2)$ and $n_{i\sigma\alpha} = c_{i\sigma\alpha}^\dagger c_{i\sigma\alpha}$. The nearest and next nearest neighbor intralayer tunneling amplitudes between sites i and j are denoted by t_{ij}. The chemical potential μ controls the doping; V_{ij} are the attractive interactions. The interlayer coupling strengths g_{ij} are assumed to decay exponentially with distance $r_{ij} = \sqrt{d^2 + \rho_{ij}^2}$ as

$$g_{ij} = g_0 e^{-(r_{ij}-d)/\zeta}, \quad (6)$$

where ρ_{ij} is the in-plane separation between sites i and j, d is the distance between the monolayers, and ζ denotes the characteristic length scale for interlayer tunneling.

For simplicity and concreteness, we will focus here on a specific commensurate twist angle $\theta_{1,2} = 2 \arctan(1/2) \simeq 53.13°$, which leads to the smallest nontrivial moiré unit cell with 10 sites, as sketched in Fig. 1, and is sufficiently close to 45° to illustrate all the interesting physics. We will refer to this lattice model as the 10-band model in the following. In the SM, we show the Kerr angle results for other commensurate twist angles that are computationally accessible.

The phase diagram of the 10-band model, obtained through the standard mean-field decoupling of the interaction term in the pairing channel and then solving the resulting gap equations [13], is displayed in Fig. 2(b). At weak interlayer coupling g_0, we find that d-wave superconducting order parameters in twisted monolayers acquire a complex relative phase, spontaneously breaking the time reversal symmetry and forming a $d + id'$ TSC. This phase is characterized by Chern number $C = 4$, which can be understood as two layers of $d + id'$ TSC, each contributing $C = 2$. As g_0 gets stronger, the system transitions into the $\mathcal{T}$-broken but topologically trivial $d + is$ state with $C = 0$. For even larger g_0, the complex phase between layers disappears, resulting in a gapless phase that can be thought of as two independent $d_{x^2-y^2}$ superconductors in the band basis. We note that for twist angles closer to 45°, the gapless phase is replaced by another TSC phase characterized by
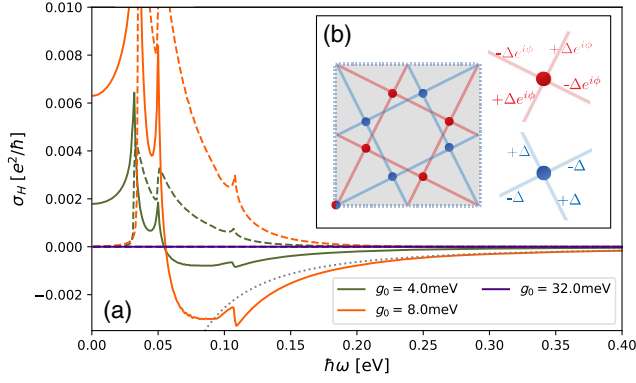
FIG. 1. (a) Optical Hall conductivity for the 10-band lattice model calculated from Eq. (4) for various values of the interlayer coupling strength g_0. Solid and dashed lines show the real and the imaginary parts of $\sigma_H(\omega)$, respectively. The tight binding model parameters are chosen to be $t = 0.153$ eV, $t' = -0.45\ t$, $\mu = -1.3\ t$. The superconducting order parameter is calculated self consistently with V_{ij} chosen such that the maximum gap is 40 meV. Gray dotted curve shows the ω^{-2} scaling that is the expected behavior of $\mathrm{Re}\sigma_H(\omega)$ in the high frequency limit. (b) The 10-band model unit cell with two stacked layers is depicted in blue and red. The signs characteristic of d-wave order parameter along with the relative complex phases are indicated in the right panel. Note that the complex phases in the order parameters break the mirror reflection symmetries along the x, y, and $x \pm y$ directions.

$C = 2$ [13]. This can be regarded as a single-layer $d + id'$ superconductor in the band basis.

Figure 1 shows our results for the Hall conductivity $\sigma_H(\omega)$ in the 10-band model computed using Eq. (4). The
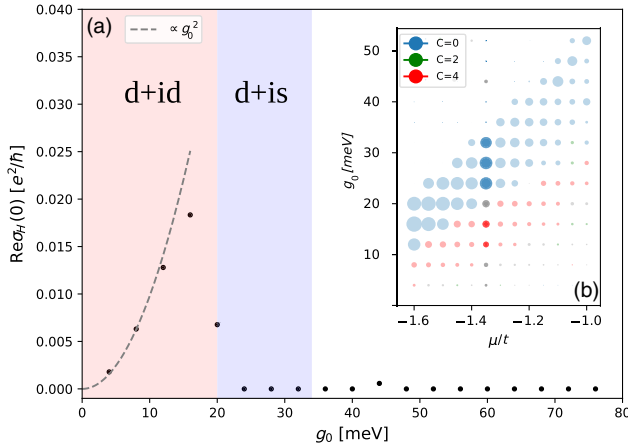

FIG. 2. (a) Zero frequency limit of the real part of the optical Hall conductivity $\sigma_H(\omega)$ for the 10-band lattice model for the same parameters as Fig. 1. The data shown in the main panel corresponds to the highlighted slice in the inset, (b), which displays the phase diagram of this configuration as a function of g_0 and μ/t. The color corresponds to the Chern number C, while the radius of the dots is proportional to the minimum excitation gap.

parameters are chosen to capture $Bi_2Sr_2CaCu_2O_{8+\delta}$ near optimal doping, where we expect the mean-field BCS theory to provide an accurate description of the super-conducting state. Because the strength of the interlayer coupling g_0 is difficult to accurately estimate for the twisted configuration, we display $\sigma_H(\omega)$ for several representative values spanning its likely range. When $g_0 < 20$ meV, the ground state has Chern number $C = 4$. The Hall conductivity is nonzero with an amplitude that is *3 to 4 orders* of magnitude larger than the prediction for Sr_2RuO_4 given in Ref. [17]. We show below that this leads to a giant Kerr angle that should be straightforward to detect experimentally. By contrast in the $C = 0$ phase, obtained for $g_0 = 32$ meV, $\sigma_H(\omega)$ is much smaller ($\approx 10^{-7} e^2/\hbar$) and will lead to a very weak Kerr signal.

Effective 2-band model.—In order to gain some insight into the Hall response of twisted bilayers, we now consider an effective 2-band model designed to capture the essential features of the system. The 2-band Bogoliubov–de Gennes Hamiltonian h_k^{eff} and its derivation are given in the SM. The Hall conductivity, Eq. (2), for the 2-band model is found to be

$$\sigma_H(\omega) = 2e^2 \sum_k \mathrm{Im}[\Delta_1^* \Delta_2][\partial_k(\xi_2 - \xi_1) \times \partial_k |g|^2]_z$$
$$\times \frac{1}{E_1 E_2}\left[\frac{1 - n_F(E_1) - n_F(E_2)}{E_+(E_+^2 - (\omega + i\epsilon)^2)} - \frac{n_F(E_1) - n_F(E_2)}{E_-(E_-^2 - (\omega + i\epsilon)^2)}\right],$$
(7)

where $\xi_{1(2)}$ and $\Delta_{1(2)}$ are the effective dispersions and gap functions defined in Eqs. (S8) and (S9) of the SM, $E_{1,2}$ denote the positive energy eigenvalues of h_k^{eff} and $E_\pm = E_1 \pm E_2$. The SM gives the derivation of Eq. (7) and also shows a comparison with $\sigma_H(\omega)$ obtained directly from the 10-band model.

Equation (7) is useful because it clarifies conditions under which a system can exhibit the nonvanishing anomalous Hall effect. Specifically, three physical ingredients are required in addition to broken $\mathcal{T}$ and mirror symmetries: (i) the two normal-state dispersions must be different ($\xi_1 \neq \xi_2$), (ii) a nonvanishing superconducting phase difference must exist between the layers such that $\mathrm{Im}[\Delta_1^* \Delta_2]$ is nonzero, and (iii) the interlayer coupling g must be k dependent. In the 2-band model defined by the Eq. (S7) Hamiltonian in the SM, the first two conditions are satisfied for a $d + id'$ state and when second-neighbor in-plane tunneling $\tilde{t}'$ is nonzero. The third condition will be met if we allow interlayer hopping between sites that are not directly above one another. For instance, we may assume the two square lattices to be offset by $(b/2, b/2)$ and allow nearest neighbor hopping; this gives $g(k) = 4g_0 \cos(k_x b/2) \cos(k_y b/2)$. Importantly, we expect the above conditions to be met in a physical sample of a twisted $Bi_2Sr_2CaCu_2O_{8+\delta}$ bilayer.

To produce a finite and significant Hall signal, the integrand in Eq. (7) must be even under the reflection $x \leftrightarrow y$. This is most easily ensured when all factors are even: the $\mathcal{T}$-breaking $\mathrm{Im}[\Delta_1^* \Delta_2]$, the vertex, and the energy factors are all even in the $d + id'$ case. On the other hand, $\mathrm{Im}[\Delta_1^* \Delta_2]$ becomes odd in the $d + is$ case, which renders the signal vanishing. This exemplifies a situation that breaks both mirror and time reversal symmetries but still exhibits no Kerr signal. This distinguishing feature between the two $\mathcal{T}$-breaking cases, trivial $d + is$ and topological $d + id'$, is indeed confirmed in the 10-band calculation in Fig. 2, where the former exhibits a negligibly small signal compared to the latter.

At zero temperature, only the first term on the second line of Eq. (7) contributes. This term describes a process of breaking a Cooper pair into two quasiparticles on different branches of the spectrum and indicates the onset of the absorptive part $\mathrm{Im}[\sigma_H(\omega)]$ at $\omega^* = \min_{\boldsymbol{k}}[E_1(\boldsymbol{k}) + E_2(\boldsymbol{k})]$. Note that ω^* is roughly set by the energy scale of the interlayer coupling g when the pairing is small compared to the chemical potential and is in general much larger than the quasiparticle gap minimum. We expect this physical picture and the form of ω^* to hold approximately in the 10-band model, with $E_{1,2}$ being the two lowest energy levels. This is indeed confirmed in our numerical calculations shown in Fig. 1 and Fig. S3 in the SM.

Lastly, Eq. (7) shows that the Hall signal amplitude exhibits quadratic dependence on g and Δ to leading order. This is numerically confirmed to hold in the 10-band model as indicated in Fig. 2 for the g dependence. This observation suggests a plausible explanation for why Fig. 1 shows signal 4 orders of magnitude larger than that predicted for Sr_2RuO_4 [2]: in $Bi_2Sr_2CaCu_2O_{8+\delta}$, the gap Δ is about 2 orders of magnitude larger, while g is roughly the same in the two materials.

Kerr angle estimate.—We use Eq. (1) and its thin sample $(\lambda \gg h)$ counterpart [19] given by

$$\theta_K = \mathrm{Re} \arctan\left[\frac{-\sigma_{xy}}{\sigma_{xx} + 4\pi(\sigma_{xx}^2 + \sigma_{xy}^2)} \right] \qquad (8)$$

to estimate the expected Kerr angle. Here, the optical conductivities are made dimensionless by attaching the fine structure constant α, i.e., setting $e^2/\hbar = \alpha$ in the natural units. The C_4 rotation symmetry of the twisted bilayer implies $\sigma_{xy} = -\sigma_{yx}$, which, in combination with Eq. (2), gives $\sigma_{xy} = \sigma_H$. The diagonal part of the conductivity tensor and the complex index of refraction required in Eq. (1) are dominated by various relaxation mechanisms whose microscopic origin is poorly understood in the cuprates. To estimate σ_{xx}, we thus rely on an empirical power-law formula,
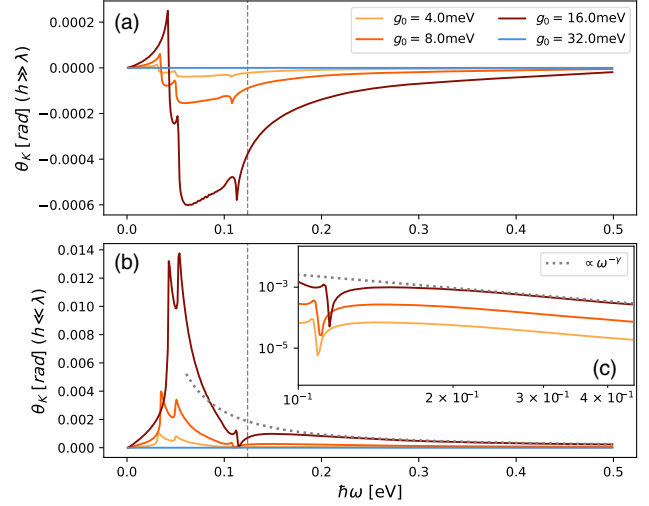

FIG. 3. Kerr angle θ_K as a function of photon energy $\hbar\omega$ for various values of interlayer coupling g_0. (a) Thick sample limit [Eq. (1)]. (b) Thin sample limit [Eq. (8)]. (c) Semilog plot with the expected $\omega^{-\gamma}$ scaling at high frequencies shown by the dotted gray line. Vertical dashed lines indicate the frequency ω_c above which σ_{xx} shows the power-law form $\propto (-i\omega)^{\gamma-2}$.

$$\sigma_{xx} \simeq 2dC(-i\omega)^{\gamma-2}, \qquad \gamma = 1.447, \qquad (9)$$

that was shown in Ref. [21] to accurately describe the ab-plane reflectance data on $Bi_2Sr_2CaCu_2O_{8+\delta}$ for frequencies above $\omega_c \simeq 0.12$ eV at all temperatures. System thickness $h = 2d$ is inserted to convert between the bulk and thin film conductivity.

Figure 3 shows our results for PKE with further details provided in the SM. For simplicity, we assume the power law, Eq. (9), to be valid at all frequencies and therefore expect our predictions for θ_K to be less accurate for $\omega \lesssim \omega_c$. We note, however, that PKE experiments are typically performed at frequencies above ~ 0.5 eV [4,15], well within the range of the applicability of Eq. (9).

In this experimentally relevant regime, it is possible to obtain a simple approximate expression for θ_K in the thin sample limit that can be used as guidance in experimental studies. As shown in the SM for $\omega \gtrsim \omega_c$, one may approximate Eq. (8) as

$$\theta_K \simeq \Lambda g_0^2 \omega^{-\gamma}, \qquad (10)$$

where θ_K is in radians and $\Lambda = 0.3623$ [eV]$^{\gamma-2}$ is a constant we extract by fitting the curves in Fig. 3, which show excellent agreement with the scaling form, Eq. (10). For the typical photon frequency $\hbar\omega = 0.5$ eV, Eq. (10) predicts $\theta_K \simeq 10$–100 μrad if we assume $g_0 = 4$–16 meV.

Summary and conclusions.—Our modeling predicts a large *intrinsic* contribution to the anomalous Hall conductivity of twisted $Bi_2Sr_2CaCu_2O_{8+\delta}$ bilayer in the spontaneously $\mathcal{T}$-broken topological phase, which is expected to occur for a range of twist angles close to 45°. There could

be other "extrinsic" contributions to $\sigma_H(\omega)$ from various scattering mechanisms discussed in the literature [22–25] that we have not considered here. Typically, such contributions arise from higher-order diagrams in the expansion of the current-current correlator [Eq. (3)] and are thus subdominant with respect to the intrinsic component identified here. To the extent that various contributions are additive, our estimate for the Kerr angle should therefore be viewed as a lower bound. Its large magnitude, measured in μrad rather than nrad, typical of Sr_2RuO_4 and other chiral SC candidates such as UPt_3 [26,27], gives hope that spontaneous $\mathcal{T}$ breaking in twisted high-T_c cuprate bilayers can be reliably and unambiguously detected with existing laboratory instruments.

---

*These authors contributed equally to this work.

[1] É. Lantagne-Hurtubise and M. Franz, Topology in abundance, Nat. Rev. Phys. **1**, 183 (2019).

[2] C. Kallin and J. Berlinsky, Chiral superconductors, Rep. Prog. Phys. **79**, 054502 (2016).

[3] G. M. Luke, Y. Fudamoto, K. M. Kojima, M. I. Larkin, J. Merrin, B. Nachumi, Y. J. Uemura, Y. Maeno, Z. Q. Mao, Y. Mori, H. Nakamura, and M. Sigrist, Time-reversal symmetry-breaking superconductivity in Sr_2RuO_4, Nature (London) **394**, 558 (1998).

[4] J. Xia, Y. Maeno, P. T. Beyersdorf, M. M. Fejer, and A. Kapitulnik, High Resolution Polar Kerr Effect Measurements of Sr_2RuO_4: Evidence for Broken Time-Reversal Symmetry in the Superconducting State, Phys. Rev. Lett. **97**, 167002 (2006).

[5] A. Pustogow, Y. Luo, A. Chronister, Y.-S. Su, D. A. Sokolov, F. Jerzembeck, A. P. Mackenzie, C. W. Hicks, N. Kikugawa, S. Raghu, E. D. Bauer, and S. E. Brown, Constraints on the superconducting order parameter in Sr_2RuO_4 from oxygen-17 nuclear magnetic resonance, Nature (London) **574**, 72 (2019).

[6] P. Zhang, K. Yaji, T. Hashimoto, Y. Ota, T. Kondo, K. Okazaki, Z. Wang, J. Wen, G. D. Gu, H. Ding, and S. Shin, Observation of topological superconductivity on the surface of an iron-based superconductor, Science **360**, 182 (2018).

[7] M. Kriener, K. Segawa, Z. Ren, S. Sasaki, and Y. Ando, Bulk Superconducting Phase with a Full Energy Gap in the Doped Topological Insulator $Cu_xBi_2Se_3$, Phys. Rev. Lett. **106**, 127004 (2011).

[8] V. Mourik, K. Zuo, S. M. Frolov, S. R. Plissard, E. P. A. M. Bakkers, and L. P. Kouwenhoven, Signatures of majorana fermions in hybrid superconductor-semiconductor nanowire devices, Science **336**, 1003 (2012).

[9] A. Das, Y. Ronen, Y. Most, Y. Oreg, M. Heiblum, and H. Shtrikman, Zero-bias peaks and splitting in an Al–InAs nanowire topological superconductor as a signature of majorana fermions, Nat. Phys. **8**, 887 (2012).

[10] L. P. Rokhinson, X. Liu, and J. K. Furdyna, The fractional a.c. Josephson effect in a semiconductor–superconductor nanowire as a signature of majorana particles, Nat. Phys. **8**, 795 (2012).

[11] A. D. K. Finck, D. J. Van Harlingen, P. K. Mohseni, K. Jung, and X. Li, Anomalous Modulation of a Zero-Bias Peak in a Hybrid Nanowire-Superconductor Device, Phys. Rev. Lett. **110**, 126406 (2013).

[12] M. T. Deng, S. Vaitiekenas, E. B. Hansen, J. Danon, M. Leijnse, K. Flensberg, J. Nygård, P. Krogstrup, and C. M. Marcus, Majorana bound state in a coupled quantum-dot hybrid-nanowire system, Science **354**, 1557 (2016).

[13] O. Can, T. Tummuru, R. P. Day, I. Elfimov, A. Damascelli, and M. Franz, High-temperature topological superconductivity in twisted double-layer copper oxides, Nat. Phys. **17**, 519 (2021).

[14] P. A. Volkov, J. H. Wilson, and J. H. Pixley, Magic angles and current-induced topology in twisted nodal superconductors, arXiv:2012.07860.

[15] A. Kapitulnik, J. Xia, E. Schemm, and A. Palevski, Polar Kerr effect as probe for time-reversal symmetry breaking in unconventional superconductors, New J. Phys. **11**, 055060 (2009).

[16] Y. Wang, A. Chubukov, and R. Nandkishore, Polar Kerr effect from chiral-nematic charge order, Phys. Rev. B **90**, 205130 (2014).

[17] E. Taylor and C. Kallin, Intrinsic Hall Effect in a Multiband Chiral Superconductor in the Absence of an External Magnetic Field, Phys. Rev. Lett. **108**, 157001 (2012).

[18] P. N. Argyres, Theory of the Faraday and Kerr effects in ferromagnetics, Phys. Rev. **97**, 334 (1955).

[19] W.-K. Tse and A. H. MacDonald, Magneto-optical Faraday and Kerr effects in topological insulator films and in other layered quantized hall systems, Phys. Rev. B **84**, 205327 (2011).

[20] See Supplemental Material at http://link.aps.org/supplemental/10.1103/PhysRevLett.127.157001 for the derivation of the 2-band model, a comparison of 2-band and 10-band models, details of the numerical estimate of Kerr rotation angle and the derivation of the optical Hall conductivity formula used in numerical calculations.

[21] J. Hwang, T. Timusk, and G. D. Gu, Doping dependent optical properties of $Bi_2Sr_2CaCu_2O_8 + \delta$, J. Phys. Condens. Matter **19**, 125208 (2007).

[22] S. K. Yip and J. A. Sauls, Circular dichroism and birefringence in unconventional superconductors, J. Low Temp. Phys. **86**, 257 (1992).

[23] R. Roy and C. Kallin, Collective modes and electromagnetic response of a chiral superconductor, Phys. Rev. B **77**, 174513 (2008).

[24] J. Goryo, Impurity-induced polar Kerr effect in a chiral p-wave superconductor, Phys. Rev. B **78**, 060501(R) (2008).

[25] R. M. Lutchyn, P. Nagornykh, and V. M. Yakovenko, Frequency and temperature dependence of the anomalous ac Hall conductivity in a chiral $p_x + ip_y$ superconductor with impurities, Phys. Rev. B **80**, 104508 (2009).

[26] E. R. Schemm, W. J. Gannon, C. M. Wishne, W. P. Halperin, and A. Kapitulnik, Observation of broken time-reversal symmetry in the heavy-fermion superconductor UPt3, Science **345**, 190 (2014).

[27] Z. Wang, J. Berlinsky, G. Zwicknagl, and C. Kallin, Intrinsic ac anomalous Hall effect of nonsymmorphic chiral superconductors with an application to UPt_3, Phys. Rev. B **96**, 174511 (2017).